SCIENCE CHINA
Chemistry

•ARTICLES•

April 2018 Vol.61 No.4: 483–489
https://doi.org/10.1007/s11426-017-9194-6

Super-resolution imaging and real-time tracking lysosome in living cells by a fluorescent probe

Wencheng Zhu[1,3†], Xujun Zheng[2†], Yan Huang[2], Zhiyun Lu[2*] & Hua Ai[1*]

[1]*National Engineering Research Center for Biomaterials, Sichuan University, Chengdu 610064, China;*
[2]*Key Laboratory of Green Chemistry and Technology, Ministry of Education; College of Chemistry, Sichuan University, Chengdu 610064, China;*
[3]*Shanghai Institute of Biochemistry and Cell Biology, Chinese Academy of Sciences, Shanghai 200031, China*

Received October 12, 2017; accepted December 15, 2017; published online January 24, 2018

Lysosomes function as important organelles within cells and their movement associates with diverse biological events, hence the real-time tracking of lysosomal movement is of great significance. However, since most lysosome fluorescent probes suffer from relatively unsatisfactory photostability, tracking lysosomal movement in real-time remains challenging. Here, we report that a naphthalimide-based fluorescent compound, namely NIMS, is a quite promising probe for lysosome imaging. The visualizing mechanism lies in the selective accumulation of NIMS in lysosomes via a protonation reaction, followed by the fluorescence enhancement due to the interactions of NIMS with proteins. Owing to its high selectivity and good photostability, NIMS was successfully applied to capture super-resolution fluorescence images of lysosomes. More importantly, real-time tracking of lysosome movement in a single living cell by NIMS was realized with a confocal laser scanning microscope. Surprisingly, even in normal culture conditions, around 2/3 of the captured lysosomes were observed to move within 5 min, indicative of the highly dynamic features of lysosomes. Thus, this probe may facilitate the understanding of the lysosome dynamics in physiological or pathological conditions.

lysosome imaging, protonation, photostability, naphthalimide

Citation: Zhu W, Zheng X, Huang Y, Lu Z, Ai H. Super-resolution imaging and real-time tracking lysosome in living cells by a fluorescent probe. *Sci China Chem*, 2018, 61: 483–489, https://doi.org/10.1007/s11426-017-9194-6

1 Introduction

Lysosomes, regarded as the "stomach" of a cell, play essential roles in recycling of intracellular organic materials and clearance of endocytosed materials [1,2]. In human body, the dysfunction of lysosomes not only leads to various lysosomal storage diseases, but also is associated with inflammation and tumor [3,4]. Recently, it was found that the positioning of lysosomes could be precisely controlled to meet the changing cellular needs. For example, under nutrient deprivation conditions, lysosomes could be rapidly recruited to the perinuclear region [5]. Therefore, visual labelling and tracking of lysosome would be significantly helpful to understand lysosomal working principles [3], intracellular metabolism [4] and cell membrane recycling status [6], and the evaluation of drug and gene delivery systems as well [7,8]. More importantly, recording of dynamic lysosomal movement in a real-time manner would facilitate the understanding of where lysosomes work and what kinds of organelles lysosomes could interact with. However, the photo-instability of small-molecule fluorescent lysosome probes limits the monitoring window for real-time tracking. In fact, so far there are only a few reports on the

†These authors contributed equally to this work.
*Corresponding authors (email: luzhiyun@scu.edu.cn; huaai@scu.edu.cn)

study of lysosomal dynamics in real time [9,10], and the development of novel high-performance fluorescent probes for real-time monitoring of lysosomes is important but challenging.

To date many kinds of small molecular lysosome fluorescent probes have been successfully developed. Their signalling principle usually lies in the selective targeting followed by visualizing processes of them towards lysosomes. To endow the fluorophores with lysosomal targeting capability, most current small molecule lysosome probes bear a weakly basic subunit, thereby being accumulated in the acidic environments of lysosomes (pH 4.5–5.0) through protonation [11,12]. To realize the visualization of lysosomes, two strategies are generally employed: (1) using compounds whose fluorescence is weak in basic and neutral condition but could be "turn on" in acidic environments (e.g., commercially available LysoSensor™ pH Indicators) [13–18]; (2) using fluorescent compounds whose photoluminescence (PL) intensity is pH-independent (e.g., the commercially available LysoTracker™) [19]. The visualization mechanism of lysosome probes whose PL intensity is pH-dependent has been well-elucidated, whilst it is not clear so far for lysosome-tracking compounds whose PL intensity is pH-independent. Consequently, in-depth understanding on the visualization mechanism should be important for the exploitation of novel high-performance lysosome probes.

Recently, super-resolution fluorescence microscopy techniques, including structured illumination microscope (SIM) [20], have been widely applied on the observation of many biological structures. With the aid of fluorescent probes, the applications of super-resolution microscopes have been remarkably expanded [21,22] in cellular imaging of organelles and cellular structures, such as mitochondria [23], endoplasmic reticulum (ER) [24], lipid droplets (LDs) [25] and telomere [26]. Nevertheless, as far as lysosomes are concerned, there were only a few reports on the visualization of them through a super-resolution microscope [27–29]. To meet the criteria for super-resolution imaging, the fluorescent probe needs to be both highly selective and photostable [22,23]. Therefore, super-resolution imaging of lysosomes in living cells via small molecular fluorescent probes remains challenging.

Herein, we report our findings that a compound NIMS we developed recently, namely [(*E*)-6-(4-((*tert*-butyldiphenylsilyl)oxy)styryl)-2-(2-(dimethylamino) ethyl)-1*H*-benzo[*de*]isoquinoline-1,3(2*H*)-dione] [30] (structure shown in Scheme 1), could act as a high-performance lysosome probe. Owing to its high selectivity, good photostability and low cytotoxicity, NIMS could be applied in super-resolution imaging of lysosome and real-time tracking of lysosomal movement in living cells. Meanwhile, our results demonstrate that the signaling mechanism of NIMS towards lysosome involves an accumulation process of NIMS in lysosomes due to the protonation of its dimethylamino group in acidic environments, and a fluorescence enhancement process of NIMS due to its interactions with proteins. This mechanism might be helpful for the rational construction of high-performance lysosome fluorescent probes.

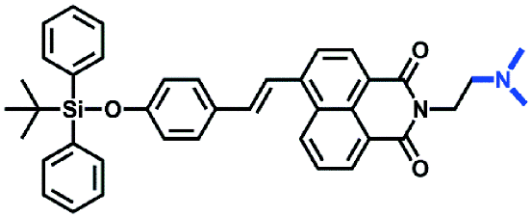

Scheme 1 Molecular structure of NIMS (color online).

2 Materials and method

2.1 Materials

Fetal bovine serum (FBS), Dulbecco's modified Eagle medium (DMEM), Roswell Park Memorial Institute-1640 medium (RPMI-1640) and trypsin-ethylenediaminetetraacetic acid (EDTA) were purchased from Gibco (USA). Phosphate-buffered saline solution (PBS, pH 7.4) and antibiotics (100 unit/mL streptomycin and 100 μg/mL penicillin) were purchased from Invitrogen (USA). RAW264.7 cells (mouse macrophage) were purchased from West China School of Pharmacy Sichuan University (Chengdu, China). HeLa (human cervical cancer cell) and MEF (mouse embryo fibroblast) cell lines were purchased from American Type Culture Collection (ATCC, USA). LysoTracker Red DND-99 was purchased from Life Technologies (USA). Chloroquine was purchased from Sigma (USA).

2.2 Cell culture

The cells were cultured as described before [31–33]. HeLa and MEF cells were cultured in DMEM supplemented with 10% FBS and 1% penicillin-streptomycin; RAW264.7 cells were cultured in RPMI-1640 supplemented with 10% FBS and 1% penicillin-streptomycin. All cells were incubated in a humidified 5% CO_2 incubator at 37 °C with the medium changed every other day.

2.3 Fluorescence imaging of lysosome by NIMS

The cells (HeLa, MEF and RAW264.7) were seeded in 35 mm glass-bottom culture dishes at a density of 1×10^5 cells per dish and incubated in a CO_2 incubator. After 24 h culture, the growth medium was removed and the fresh growth medium containing 5 μM NIMS was added into the dishes and kept for 1.5 h, then LysoTracker Red DND-99 was added (final concentration: 50 nM) and kept for another 0.5 h. After

that, the medium was removed and cells were washed with PBS twice, then 1.5 mL fresh medium was added into the dishes. Under a fluorescence microscope (Leica, Germany), NIMS was excited at blue channel (475–495 nm), while LysoTracker was excited at green channel (505–535 nm), and the pictures of cellular imaging were captured. The fluorescence signal intensity of NIMS and LysoTracker were quantified by ImageJ software (Version 1.8.0).

2.4 Fluorescence stability evaluation

RAW264.7 cells were seeded and cultured as described above. After 24 h culture, cells were stained with 5 μM NIMS for 1.5 h followed by 50 nM LysoTracker for another 0.5 h in a CO_2 incubator. Then the medium was removed and cells were incubated with fresh medium. Under a confocal laser scanning microscope (CLSM, Leica, Germany), NIMS and LysoTracker were excited at 488 and 561 nm, respectively. Cells from three different zones were scanned every 30 s (totally 5 min) with 3% laser power. The images of before and after the scanning were captured.

2.5 Super-resolution microscope imaging

HeLa cells were seeded and cultured as described above. After 12 h incubation, cells were incubated with 5 μM NIMS for 2 h. After that, the medium was removed and cells were washed with PBS twice, then 1.5 mL growth medium was added into the dishes. Under a structured illumination microscope (Nikon, Japan), NIMS was excited at 488 nm, and the pictures of cellular imaging were captured. The 3D surface plot of lysosomes was generated by ImageJ software (Version 1.8.0).

2.6 Tracking lysosome movement in living cells

MEF cells were seeded and cultured as described above. After 24 h culture, the growth medium was removed and the fresh growth medium containing 5 μM NIMS was added into the dishes. 2 h later, the medium was removed and the fresh medium was added into dishes. Then under a CLSM, NIMS was excited at 488 nm. The movement of lysosomes was captured every 15 s (totally 5 min) and the movie was made based on the pictures.

3 Results and discussion

3.1 Lysosome imaging by NIMS in different types of cells

Lysosomes are spherical vesicles distributed in the cytoplasm. First, to test the selectivity and imaging ability of NIMS towards lysosome, we selected three typical cell lines, HeLa (cancer cell), MEF (fibroblast) and RAW264.7 (macrophage), to perform the cellular imaging. As shown in Figure 1, bright fluorescence spots originated from NIMS

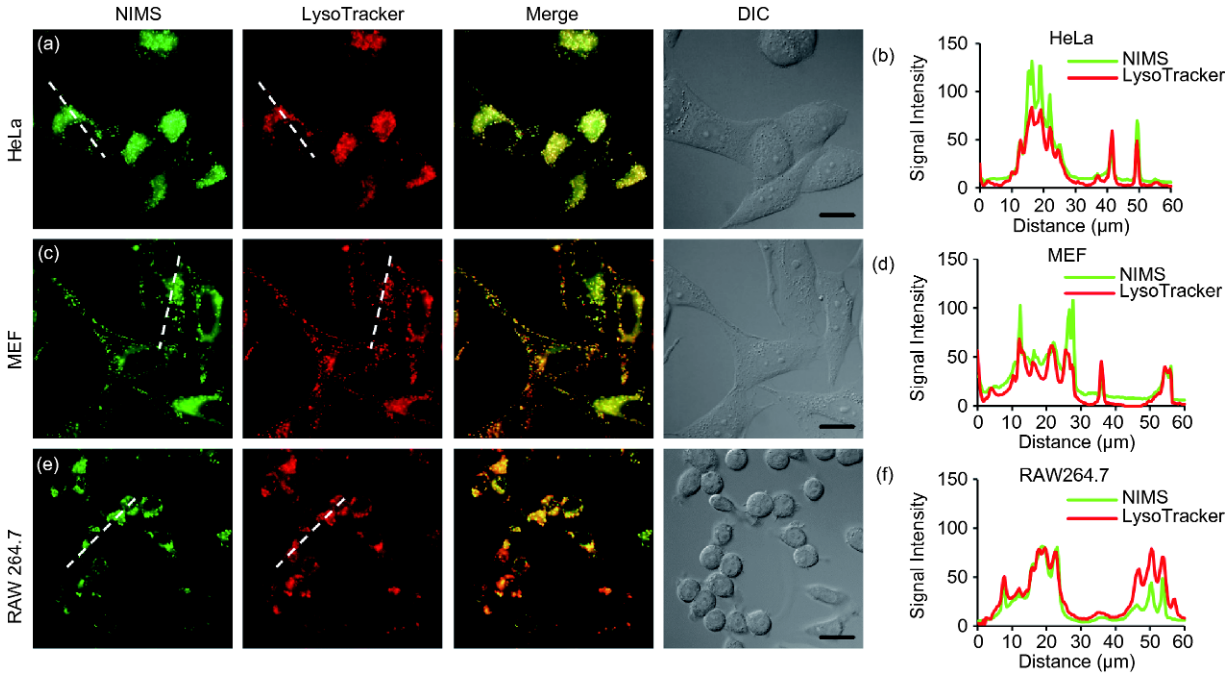

Figure 1 Fluorescence microscope images of different types of cells co-incubated with NIMS (5 μM, 2 h) and LysoTracker DND-99 (50 nM, 0.5 h). (a) HeLa cells; (c) MEF cells; (e) RAW264.7 cells. (b, d, f) The intensity profile of regions of interest (the dotted lines in (a, c, e)) cross the cells. Cells were excited at blue (475–495 nm, NIMS) or green (505–535 nm, LysoTracker) channels under a fluorescence microscope (Leica, Germany). NIMS was displayed in pseudo-color (green) to better show the colorization results. Scale bar: 20 μm (color online).

could be observed in the cytoplasm of all these cells. Meanwhile, the fluorescence signals of NIMS could be nicely co-localized with the commercial reference dye for lysosome (LysoTracker DND-99) in all these cells (Figure 1, merged pictures). In addition, the fluorescence signal intensity profiles of the two dyes were found to be highly correlated (Figure 1(b, d, f)). Based on these observations, it could be inferred that NIMS can act as a highly selective lysosome probe capable of labeling lysosomes in cellular imaging applications.

3.2 Accumulation of NIMS in lysosomes through protonation

To gain insight to the reason why NIMS could target lysosomes, additional chloroquine (CQ) pre- and post-treatment experiments (50 μM, 0.5 h) were conducted on the NIMS and LysoTracker co-incubated HeLa cells, since the CQ treatment on cells will lead to inhibited lysosomal acidification process, thereby elevating lysosomal pH [13,34]. As shown in Figure S1 (Supporting Information onine), in comparison with the control group (lacking of CQ treatment), the CQ pre-treatment on the NIMS and LysoTracker co-incubated cells was found to result in much weakened fluorescence, but the CQ post-treatment has negligible influence on the fluorescence intensity of these NIMS and LysoTracker co-stained cells (Figure S1(c, f)). Consequently, the acidic microenvironments should be a perquisite for the accumulation of NIMS in lysosomes; yet after being accumulated successfully in lysosomes, the elevated pH of lysosomes will no longer have significant effects on both the cellular localization and the fluorescence intensity of NIMS. Similar phenomenon could be observed for LysoTracker (Figure S1(f)) and other reported probes [11,34], confirming that all these probes should be accumulated successfully in lysosomes through protonation processes on their alkaline moities in the acidic microenvironment of lysosomes [35].

Further time-course imaging experiments of NIMS-stained cells (0–3 h, shown in Figure S1(g)) revealed that with increasing incubation time, the PL intensity of NIMS-stained cells increases progressively, confirming the presence of accumulation behaviors of NIMS in the cells.

3.3 Fluorescence enhancement of NIMS in the presence of proteins

Despite the fact that NIMS-incubated cells could emit intense fluorescence, the NIMS solutions in aqueous PBS just exhibits quite weak PL emission (Figure S2(a)). Taking into consideration that NIMS is a luminogen showing intramolecular charge-transfer (ICT) transition character, the much enhanced fluorescence of NIMS in intracellular environments might arise from its interactions with bio-macromolecules like proteins whose microenvironments are less polar than water [36–41]. In fact, our previous work has revealed that the PL intensity of NIM, an analog of NIMS, could be enhanced in the presence of proteins in acidic environments [34], thus we investigated the fluorescence behaviors of NIMS in PBS solution upon addition of BSA (bovine serum albumin). Based on the fact that the protein concentration within cell is around 7% (*w*/*v*) [42], 5% BSA (*w*/*v*) was used to mimic the intracellular protein environment. As shown in Figure S2(a), with increasing NIMS concentrations, the fluorescence was intensified gradually; with increasing BSA concentrations, the PL intensity of NIMS was also enhanced gradually (Figure S2(b)). These observations indicate that the interactions between NIMS and proteins could trigger distinct fluorescence enhancement, which might be attributed to the less polar microenvironments than water around NIMS.

To verify this deduction, the fluorescence behaviors of formaldehyde-fixed (dead) HeLa cells co-incubated with NIMS were studied, because the fix of cells by 4% formaldehyde solution would lead to completely disrupted acidic environments of cellular lysosomes [34]. As shown in Figure S2(c), the fluorescence of NIMS was discernable in the dye-incubated cells. In addition, unlike those NIMS-stained living cells whose fluorescence is merely localized in lysosomes, the NIMS-incubated fixed cells have their fluorescence distributed in the whole cellular regions lacking of spot-shaped character. Taking into consideration that the formaldehyde-fixation of cells will lead to damaged cell structure hence more uptake of NIMS, it could be inferred from these observations that the acidic environment should be an indispensable condition for NIMS to visualize lysosomes.

In light of these experimental observations, we tentatively proposed the visualizing mechanism of NIMS to lysosome as following: (1) the specific accumulation of NIMS in lysosomes due to the protonation of its dimethylamino group in acidic environments; (2) the fluorescence enhancement of NIMS due to its interactions with bio-macromolecules with less polar microenvironments than water. Note that the protein-enhanced fluorescence uncovers an additional step of lysosome visualization during the function of lysosome probe in cellular microenvironment. Hence, our findings might be helpful for the better understanding of the lysosome probe visualization mechanisms and the development of high-performance lysosome fluorescent probes.

3.4 Photostability and cytotoxicity of NIMS in cellular imaging

Besides selectivity, photostability is considered as one of the key factors in evaluating the performance of fluorescent imaging probes. The photostability of RAW264.7 cells co-

stained with NIMS and LysoTracker was investigated by monitoring the fluorescence intensity before and after continuously being scanned for 11 times by confocal microscopy. After 5 min imaging under the CLSM, the fluorescent intensity of LysoTracker in RAW264.7 cells was observed to drop much more quickly and dramatically than that of NIMS (Figure 2(a–d)). As shown in Figure 2(e), even after 1 min excitation, the PL intensity of the LysoTracker-stained cells was reduced by about 80%; meanwhile the intensity loss of NIMS-based samples is less than 20%. Furthermore, after the total 11 scans with an entire excitation time of 5 min, the fluorescence intensity of NIMS-based samples still remained about 30%; in contrast, that of LysoTracker-based samples was nearly undetectable, and was less than 10% (Figure 2(d, e)). Therefore, NIMS should possess better photostability than commercially available LysoTracker during the cellular imaging of lysosomes.

In addition, we measured the cytotoxicity of NIMS in HeLa and MEF cells by a standard CCK-8 assay. As shown in Figure 3, after 24 h incubation with NIMS, these cells only showed a slight growth inhibition at high concentrations of NIMS indicating the cytotoxicity of NIMS is low.

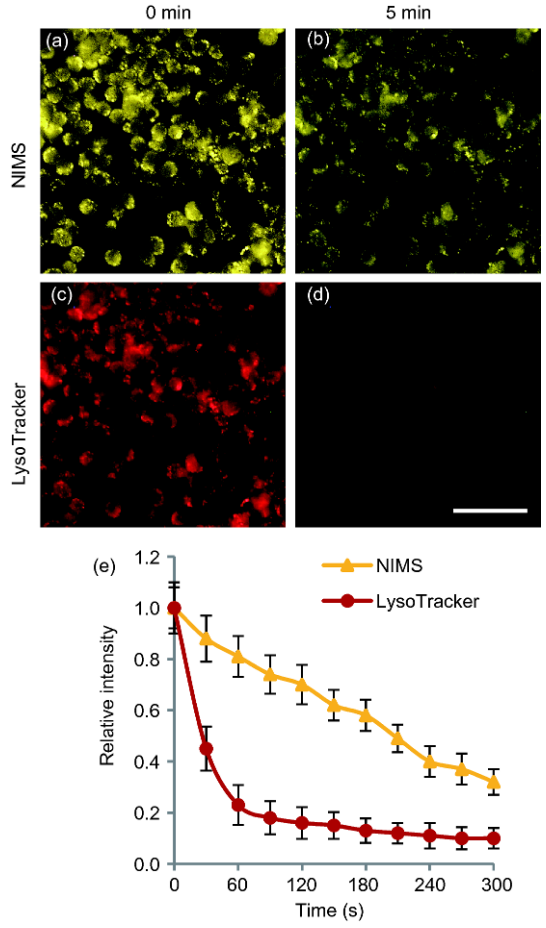

Figure 2 Photostability of NIMS in cellular imaging. Fluorescent images of NIMS and LysoTracker co-stained RAW264.7 cells, the fluorescence of NIMS before (a) and after (b) the scanning; the fluorescence of LysoTracker before (c) and after (d) the scanning; (e) relative fluorescence intensity of NIMS and LysoTracker during the scanning (n=3). Error bar represents standard deviation (SD). Scale bar: 100 μm (color online).

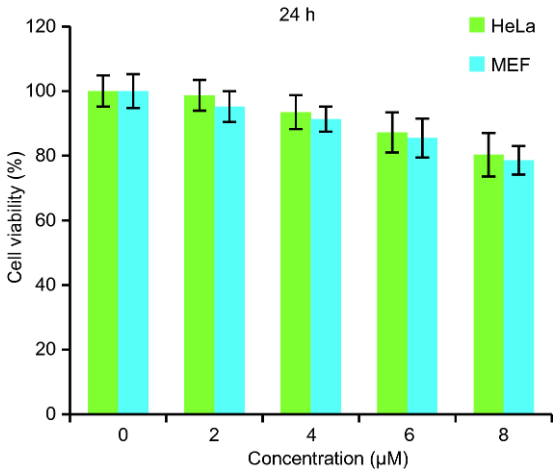

Figure 3 Cytotoxicity of NIMS in HeLa and MEF cells. The cells were treated with different concentrations of NIMS for 24 h, then the cell viability was determined by CCK-8 assay (color online).

3.5 Super-resolution fluorescence imaging lysosomes by NIMS

Recently, with the aid of super-resolution fluorescence microscope that is capable of overcoming the diffraction limit in traditional microscope, the understanding on the working pattern of organelles and proteins in cell biology was greatly enhanced. Since NIMS displays high selectivity and good photostability, which meet two of the key criteria of fluorescent probes for super-resolution imaging, we tried to visualize lysosomes by NIMS under a structured illumination microscope (SIM). As illustrated in Figure 4(a), a super-resolution image of lysosomes in a living HeLa cell was obtained successfully. In comparison with fluorescence microscope or CLSM images, the SIM picture showed a more detailed size and morphology of lysosomes. Moreover, the SIM image was used to generate a 3D surface plot of the fluorescence intensity of lysosomes (Figure 4(b)), which displays the signal intensity and distribution of lysosomes in cytoplasm.

3.6 Tracking lysosome movement by NIMS at the single-cell level

The functions of lysosomes are tightly associated with their movement. For example, in phagocytes, the lysosome movement plays essential roles in the bactericidal activities and trans-matrix migration of the cell [43]. To monitor lysosomal movement, the fluorescence probe needs to be highly selective and relatively photostable. As the reported lysosome-targeting fluorescent probes often suffer from relatively unsatisfactory photostability, so far only few probes

or dyes were demonstrated to be capable of monitoring the movement of lysosomes in real-time imaging [9,10]. Taking advantage of its high selectivity and good photostability, we employed NIMS as the lysosome-targeting probe and carried out real-time cell imaging experiments under a CLSM. As shown in Figure 5(a–h), after being stained by NIMS, the moving of lysosomes in a single living cell can be readily captured by the microscope. Surprisingly, within 5 min, 22 out of the 36 captured lysosomes in the cell were observed to move under normal culture conditions (Figure 5(i), and the Movie S1 in the Supporting Information online). Interestingly, four of the lysosomes were observed to move together

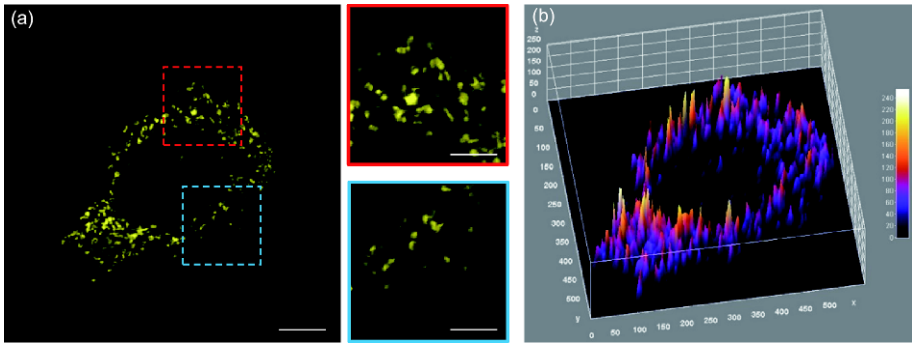

Figure 4 Super-resolution imaging lysosomes in HeLa cells by NIMS (5 μM, 2 h). (a) A picture of structured illumination microscopy (SIM) imaging lysosomes in a living HeLa cell (scale bar: 10 μm). The insets are the enlarged images of the red and blue regions (scale bar: 5 μm). (b) 3D surface plot profiling of the SIM picture of lysosomes with pseudo-color representing relative fluorescence intensity (color online).

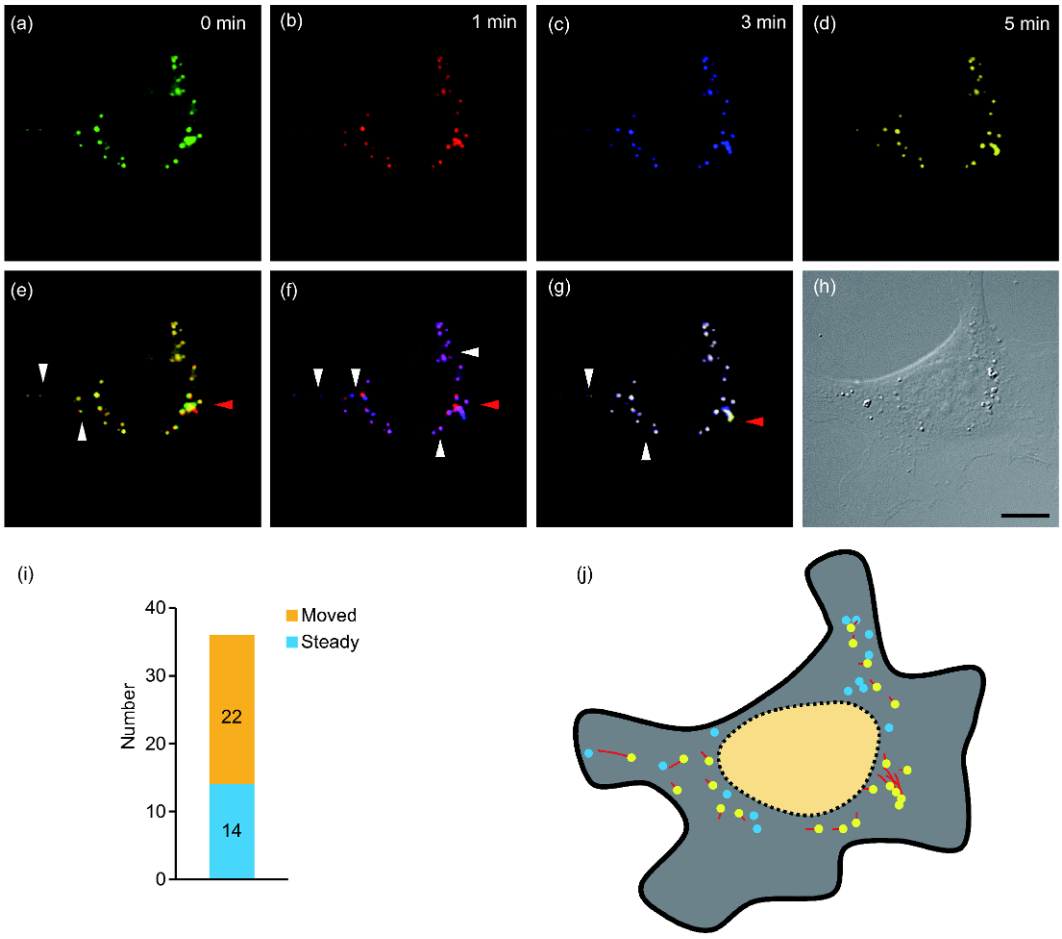

Figure 5 Real-time tracking lysosomal movement in MEF cells by NIMS (5 μM, 2 h) under CLSM. (a–d) Different pseudo-colors are used to display the movement of lysosomes at different time points (0, 1, 3, and 5 min). Merging images at two different time points: (e) 0 and 1 min, (f) 1 and 3 min, (g) 3 and 5 min; (h) DIC image of the observed cell. Scale bar: 10 μm. Arrow heads indicate the moving lysosomes. (i) Summary of the mobile status of observed lysosomes. (j) Schematic depiction of tracking lysosomal movement with NIMS. Yellow dots represent moved lysosomes with the moving route in red line, and blue dots represent steady lysosomes (color onilne).

(red arrow head) during this period, indicating that lysosomes might be specifically coordinated by cellular signals. The schematic depiction of the observed lysosomal movement was shown in Figure 5(j), in which the yellow dots represent the moved lysosomes during the observation period, and the red lines represent the moving routes, while the blue dots represents lysosomes without obvious movement. These data indicate that the lysosomal movement is highly dynamic. Thus, our results demonstrate that NIMS is suitable for real-time tracking of lysosomal movement.

4 Conclusions

In summary, a naphthalimide-based fluorescent probe, namely NIMS, has been demonstrated as a novel probe for imaging and tracking of lysosome. NIMS not only displays high selectivity in targeting lysosomes, but also possesses enhanced photostability than the commercially available LysoTracker. As a result, NIMS is capable of capturing super-resolution images of lysosomes and tracking lysosomal movement in real-time manner. More importantly, the signaling mechanism of NIMS towards lysosome is a combination of selective accumulation and fluorescence enhancement. The dimethylamino group of NIMS could protonate in acidic environments, which results in its accumulation in lysosome. Meanwhile, due to the interactions of NIMS with bio-macromolecules like proteins, the fluorescence could be enhanced significantly. This might promote the understanding of how fluorescent probes would function within cells.

Acknowledgements This work was supported by the National Key Basic Research Program of China (2013CB933903) and National Natural Science Foundation of China (81621003, 21372168, 24672156, 51173117, 51573108).

Conflict of interest The authors declare that they have no conflict of interest.

Supporting information The supporting information is available online at http://chem.scichina.com and http://link.springer.com/journal/11426. The supporting materials are published as submitted, without typesetting or editing. The responsibility for scientific accuracy and content remains entirely with the authors.

1 Turk B, Turk D, Turk V. *Biochim Biophys Acta*, 2000, 1477: 98–111
2 Turk V, Turk B, Turk D. *EMBO J*, 2001, 20: 4629–4633
3 Jedeszko C, Sloane BF. *Biol Chem*, 2004, 385: 1017–1027
4 Fehrenbacher N, Jäättelä M. *Cancer Res*, 2005, 65: 2993–2995
5 Korolchuk VI, Saiki S, Lichtenberg M, Siddiqi FH, Roberts EA, Imarisio S, Jahreiss L, Sarkar S, Futter M, Menzies FM, O'Kane CJ, Deretic V, Rubinsztein DC. *Nat Cell Biol*, 2011, 13: 453–460
6 Teter K, Chandy G, Quiñones B, Pereyra K, Machen T, Moore HPH. *J Biol Chem*, 1998, 273: 19625–19633
7 Hu Q, Bally MB, Madden TD. *Nucleic Acids Res*, 2002, 30: 3632–3641
8 Hanaki K, Momo A, Oku T, Komoto A, Maenosono S, Yamaguchi Y, Yamamoto K. *Biochem Biophys Res Commun*, 2003, 302: 496–501
9 Ho YM, Au NPB, Wong KL, Chan CTL, Kwok WM, Law GL, Tang KK, Wong WY, Ma CHE, Lam MHW. *Chem Commun*, 2014, 50: 4161–4163
10 Grossi M, Morgunova M, Cheung S, Scholz D, Conroy E, Terrile M, Panarella A, Simpson JC, Gallagher WM, O'Shea DF. *Nat Commun*, 2016, 7: 10855
11 Fan F, Nie S, Yang D, Luo M, Shi H, Zhang YH. *Bioconjugate Chem*, 2012, 23: 1309–1317
12 Zhang X, Wang C, Han Z, Xiao Y. *ACS Appl Mater Interfaces*, 2014, 6: 21669–21676
13 Yu F, Wang Y, Zhu W, Huang Y, Yang M, Ai H, Lu Z. *RSC Adv*, 2014, 4: 36849–36853
14 Zhu W, Chai X, Wang B, Zou Y, Wang T, Meng Q, Wu Q. *Chem Commun*, 2015, 51: 9608–9611
15 Zhu H, Fan J, Xu Q, Li H, Wang J, Gao P, Peng X. *Chem Commun*, 2012, 48: 11766–11768
16 Wan Q, Chen S, Shi W, Li L, Ma H. *Angew Chem Int Ed*, 2014, 53: 10916–10920
17 Zhang XF, Zhang T, Shen SL, Miao JY, Zhao BX. *J Mater Chem B*, 2015, 3: 3260–3266
18 Liu X, Su Y, Tian H, Yang L, Zhang H, Song X, Foley JW. *Anal Chem*, 2017, 89: 7038–7045
19 Freundt EC, Czapiga M, Lenardo MJ. *Cell Res*, 2007, 17: 956–958
20 Hirano Y, Matsuda A, Hiraoka Y. *Microscopy*, 2015, 64: 237–249
21 Hou SG, Liang L, Deng SH, Chen JF, Huang Q, Cheng Y, Fan CH. *Sci China Chem*, 2014, 57: 100–106
22 Zhou J, Yu G, Huang F. *J Mater Chem B*, 2016, 4: 7761–7765
23 Gu X, Zhao E, Zhao T, Kang M, Gui C, Lam JWY, Du S, Loy MMT, Tang BZ. *Adv Mater*, 2016, 28: 5064–5071
24 Thompson AD, Bewersdorf J, Toomre D, Schepartz A. *Biochemistry*, 2017, 56: 5194–5201
25 Zheng X, Zhu W, Ni F, Ai H, Yang C. *Sens Actuators B*, 2018, 255: 3148–3154
26 Wang S, Deng S, Cai X, Hou S, Li J, Gao Z, Li J, Wang L, Fan C. *Sci China Chem*, 2016, 59: 1519–1524
27 Changou CA, Wolfson DL, Ahluwalia BS, Bold RJ, Kung HJ, Chuang FYS. *J Vis Exp*, 2013, e50047
28 Choi H, Son JB, Kang J, Kwon J, Kim JH, Jung M, Kim SK, Kim S, Mun JY. *Biochem Biophys Res Commun*, 2017, 493: 1129–1135
29 Wu L, Li X, Ling Y, Huang C, Jia N. *ACS Appl Mater Interfaces*, 2017, 9: 28222–28232
30 Zheng X, Zhu W, Ai H, Huang Y, Lu Z. *Tetrahedron Lett*, 2016, 57: 5846–5849
31 Lin G, Zhu W, Yang L, Wu J, Lin B, Xu Y, Cheng Z, Xia C, Gong Q, Song B, Ai H. *Biomaterials*, 2014, 35: 9495–9507
32 Du J, Zhu W, Yang L, Wu C, Lin B, Wu J, Jin R, Shen T, Ai H. *Regen Biomater*, 2016, 3: 223–229
33 Lei Z, Zhu W, Xu S, Ding J, Wan J, Wu P. *ACS Appl Mater Interfaces*, 2016, 8: 20900–20908
34 Zheng X, Zhu W, Liu D, Ai H, Huang Y, Lu Z. *ACS Appl Mater Interfaces*, 2014, 6: 7996–8000
35 Horobin RW. *Color Technol*, 2014, 130: 155–173
36 Suzuki Y, Yokoyama K. *J Am Chem Soc*, 2005, 127: 17799–17802
37 Sunahara H, Urano Y, Kojima H, Nagano T. *J Am Chem Soc*, 2007, 129: 5597–5604
38 Zhang Y, Yue X, Kim B, Yao S, Bondar MV, Belfield KD. *ACS Appl Mater Interfaces*, 2013, 5: 8710–8717
39 Dey G, Gupta A, Mukherjee T, Gaur P, Chaudhary A, Mukhopadhyay SK, Nandi CK, Ghosh S. *ACS Appl Mater Interfaces*, 2014, 6: 10231–10237
40 Luo S, Lin J, Zhou J, Wang Y, Liu X, Huang Y, Lu Z, Hu C. *J Mater Chem C*, 2015, 3: 5259–5267
41 Zheng X, Peng Q, Lin J, Wang Y, Zhou J, Jiao Y, Bai Y, Huang Y, Li F, Liu X, Pu X, Lu Z. *J Mater Chem C*, 2015, 3: 6970–6978
42 Milo R. *BioEssays*, 2013, 35: 1050–1055
43 Labrousse AM, Meunier E, Record J, Labernadie A, Beduer A, Vieu C, Ben Safta T, Maridonneau-Parini I. *Front Immun*, 2011, 2: 51